# Collapse transition of a hydrophobic self avoiding random walk in a coarse-grained model solvent

Mathieu Gaudreault and Jorge Viñals

*Department of Physics, McGill University, Montreal, QC H3A 2T8, Canada*

(Dated: May 10, 2009)

## Abstract

In order to study solvation effects on protein folding we analyze the collapse transition of a Self Avoiding Random Walk composed of hydrophobic segments that is embedded in a lattice model of a solvent. As expected, hydrophobic interactions lead to an attractive potential of mean force among chain segments. As a consequence, the random walk in solvent undergoes a collapse transition at a higher temperature than in its absence. Chain collapse is accompanied by the formation of a region depleted of solvent around the chain. In our simulation, the depleted region at collapse is as large as our computational domain.

PACS numbers: 87.15.kr,87.11.Cc,05.40.Fb,87.15.ak

## I. INTRODUCTION

It is now well established that hydration forces play a central role in macromolecular assembly in solution. In particular, they are believed to be one of the dominant forces involved in protein folding and in the formation of protein-protein interfaces. Therefore considerable attention has been paid to the development of realistic coarse grained models of macromolecules in solution that incorporate solvent degrees of freedom. These models may account for cooperative effects that are known to be solvent mediated, but that are difficult to capture with classical surface exposure area models, or with explicit, all atom simulations. We present an analysis of the collapse transition of a weakly attractive self avoiding walk which is assumed to be composed of hydrophobic units and immersed in a coarse grained but explicit model solvent. Our results show that solvent fluctuations induce attractive interactions among the chain segments, and to a collapse transition of the self-avoiding walk at a higher temperature than the chain in isolation.

Despite the long standing observation that hydrophobic interactions are central to protein folding and protein-protein interactions, the development of models that capture hydrophobic interactions at the molecular scale remains a challenge. For example, the commonly used surface area exposure approximation in the calculation of conformational energies of polypeptide chains [1] is known to yield incorrect magnitudes of hydrophobic forces as compared to explicit solvent calculations [2]. For this and other reasons, the degree to which an implicit solvent can quantitatively capture the hydrophobic effect is still a matter of debate in the literature [3–5]. Furthermore, hydrophobic interactions are intrinsically non pairwise additive [6], fact that complicates its inclusion as an extra force in current folding or interaction algorithms. The discrepancy between implicit and explicit modeling of the solvent in folding studies has been illustrated recently in the folding of a $\beta$-hairpin in the Syriam hamster prion protein [7]. Local dewetting observed in the explicit solvent model stabilizes the fully folded hairpin, in agreement with experiment, but in contrast with an implicit solvent calculation that predicts a destabilized hairpin. Excess clustering of hydrophobic residues is predicted by the implicit solvent calculation, and seen to be independent of the total area of exposed surface (i.e., the implicit description cannot account for correlations between local density changes in the vicinity of an exposed residue and the conformation of the exposed surface).

Two intermediate scale (or coarse grained) models of hydrophobicity have been introduced in the literature by Chandler and coworkers [8–10], and by Ben-Naim [11] and Widom and coworkers [12–14]. These models incorporate spatial correlation effects that are absent in implicit models, while avoiding the computational complexity of fully explicit models. Free energy landscapes for a hydrophobic chain in a coarse grained solvent have been evaluated by Chandler and coworkers. They show that chain collapse is accompanied by a local depletion of solvent around extended hydrophobic surfaces [9]. We use in this work a modification of Widom's model of hydrophobicity to study the collapse transition of a weakly attractive self avoiding walk comprised of hydrophobic units. We find that the collapse transition temperature of the chain is shifted by the solvent, and that large chain fluctuations at collapse are correlated with solvent fluctuations.

The model of hydrophobicity that we use is equivalent to that first introduced by Ben-Naim [11] and further studied by Widom and co-workers [12–14]. We introduce a lattice model of a solvent as a two dimensional ferromagnetic Ising model subjected to an external magnetic field. Dividing space into $N = n \times n$ square cells, we assign a local spin variable $S_i$ to each $i$ cell, where $S_i = +1$ represents a cell occupied by vapor whereas $S_i = -1$ represents a cell occupied by water. Nearest neighbor cell spins interact with energy $J > 0$, and we also consider an imposed external magnetic field $H$. Lattice solvent models of this type have been derived by partial elimination of Gaussian fluctuations below the equilibrium thermal correlation length of water [15]. The magnetic field $H$ corresponds to the chemical potential in the liquid-vapor system. For standard physiological conditions, the chemical potential is only slightly shifted away from liquid-vapor coexistence ($H = 0$ in our case). The solvent alone undergoes a phase transition at the critical temperature $k_B T_c^{(s)}/J \simeq 2.269$ [16], from a disordered phase at high temperature to an ordered phase at low temperature. We are mostly concerned here with the range $T < T_c^{(s)}$ as we aim to study the coupling between chain collapse and the nucleation of a vapor domain in a bulk liquid phase.

To further define the model we require that a hydrophobic solute can be inserted into the solvent lattice only at interstitial sites between two adjacent cells with $S_i = +1$ (or vapor sites). Even in the absence of any direct interaction between the solute and the solvent, this requirement leads to an entropy decrease of the system by forcing two adjacent site to occupy the state $S_i = +1$ out of two possible states. Hydrophobicity mediated interactions follow through the analog in this model of a depletion force: two solute particles will cluster

to reduce the number of sites with $S_i = +1$ required to accommodate them. We begin by calculating the potential of mean force between two solute molecules inserted in this lattice solvent, and demonstrate that it is attractive.

We next introduce a hydrophobic chain that occupies interstitial sites in the lattice solvent. The chain is modeled as a self-avoiding random walk with weakly attractive interaction ($\epsilon < 0$) between neighboring monomers. If the lattice spacing of the square lattice of solvent molecule is $a$, the SARW occupies the interstitial lattice with spacing $b = a/\sqrt{2}$, as illustrated in figure 1(A). The Hamiltonian of the combined chain-solvent system is

$$\mathscr{H} = -J \sum_{\langle i,j \rangle} S_i S_j - H \sum_i S_i + \epsilon \sum_{\langle k,l \rangle} \delta_k \delta_l \quad , \tag{1}$$

where the first sum extends over nearest neighbors pairs of solvent cells in the two dimensional lattice, and the last sum extends over neighboring monomers of the SARW. A two dimensional SARW in isolation is known to undergo a collapse transition from an extended coil phase at high temperature to a globular collapsed state at low temperature at the critical temperature $k_B\theta/\epsilon \approx 1.5$ [17, 18]. We then study the change in this collapse transition brought about by the solvent.

## II. NUMERICAL METHOD

The equilibrium properties of the combined solvent-chain system have been computed by the Monte Carlo method. Given the high degeneracy of the solvent-chain states, we have implemented a variation of the Bortz-Kalos-Lebowitz algorithm (BKL) [19] to address transitions of both chain and solvent states. According to this method, a transition between two microscopic states is always accepted in the algorithm, but time (or iteration count) is variable, and incremented according to the given probability of occurrence of the transition in question.

For the solvent side of the simulation, we first construct a table of 10 classes associated with all possible solvent transitions. The first five classes refer to a cell that is initially in the liquid phase whereas the remaining five classes represent an initial vapor phase. A transition probability $P_v$, where $v = \{1, 2, ..., 10\}$, is attributed to each class according to the Metropolis algorithm, namely transitions for which $\Delta E_v > 0$ have $P_v = exp\,(-\beta \Delta E_s)$, where $\Delta E_s$ is the

solvent energy difference involved in the transition in question, and $P_v = 1$ otherwise. At each iteration of the BKL algorithm, we calculate the quantity $Q_v = \sum_{u=1}^{v} N_u P_u$, where $N_v$ is the number of solvent cells that belong to the $v^{th}$ class. A uniformly distributed random number $x_1$ is generated in the interval $I = [0, Q_{10}]$ and the $v^{th}$ class of the transition to be performed is identified so that $Q_{v-1} \leq x_1 < Q_v$ with $Q_0 = 0$. The chosen transition is then performed on a randomly chosen cell belonging to the $v^{th}$ class (with uniform probability) by updating the class number of this site as well as its four nearest neighbors. The simulation time variable is then incremented by $\Delta t = -ln[y_1]/Q_{10}$, where $y_1$ is a uniformly distributed random number in the interval $[0, 1]$. Iterations are repeated to achieve equilibrium.

Once the solvent is equilibrated, a hydrophobic SARW of length $L$ is immersed in it. The kinetic evolution of the chain is implemented in our Monte Carlo algorithm through the pivot method introduced by Lal [20], and extensively studied by Madras and Sokal [21]. Transitions involve a rotation of a chain segment by $\pm\pi/2$ around a monomer acting as a pivot. For a chain of length $L$, there are $4L - 2$ possible rotations. However, Madras has shown that for a given pivot it is only necessary to consider the rotation that involves the smallest segment, thereby reducing the number of possible transitions by two [22]. In order to satisfy the constraint that a hydrophobic monomer can only be accommodated in the interstitial site between two neighboring vapor cells, chain rotation is always accompanied by the motion of the accompanying vapor cells. We also use an extension of the BKL algorithm to perform chain transitions at fixed solvent configuration. At each iteration, we construct a table consisting of the $2L$ possible transitions representing a rotation of either $+\pi/2$ or $-\pi/2$ of the smallest segment of the chain around all $L$ possible pivots, given the initial conformation of the chain. The energy change $\Delta E_\nu = -J\Delta N_{11} - H\Delta N_1 + \epsilon\Delta N_p$, where $N_{11}$ and $N_1$ are the number of neighboring pairs and the number of cells in the state $S = +1$ respectively, and $N_p$ is the number of contacts between monomers along the chain. A transition probability is then assigned to each class, $P'_\nu = 1$ if $\Delta E_\nu \leq 0$ and $P'_\nu = exp\,(-\beta\Delta E_\nu)$ if $\Delta E_\nu > 0$. Transitions that violate the self avoiding condition are assigned $P'_\nu = 0$. At each iteration, we calculate the quantity $Q'_\nu = \sum_{\mu=1}^{\nu} P'_\mu$, with $\nu = \{0, 1, ..., 2L\}$, and choose the $\nu^{th}$ transition class to be performed such that $Q'_{\nu-1} \leq x_2 < Q'_\nu$, with $(Q'_0 = 0)$, and where $x_2$ is a random number uniformly distributed in $[0, Q'_{2L}]$. The selected transition is carried out and the simulation time variable is incremented by an amount $\Delta t = -ln[y_2]/Q'_{2L}$, where $y_2$ is a uniformly distributed random number in $[0, 1]$.

Typical conformations of the hydrophobic SARW in solvent are shown in Figs. 1(B,C,D).

We consider periodic boundary conditions for both the solvent and the SARW, with an initial condition for the solvent $S_i = -1$ for all $i$ (i.e. a uniform liquid phase). The initial configuration of the solvent is allowed to equilibrate up to $t = 100$ time units. A SARW of length $L$ is then inserted in the solvent. We start with a linear configuration and surround the chain with the appropriate number of vapor cells ($S_k = +1$) in order to satisfy the constraint that gives rise to hydrophobicity. The chain is then allowed to thermalize for $t = 5L^3$ time units. Following this initial equilibration, one iteration of the algorithm involves several solvent transitions at fixed chain conformation (up to 10 time units), followed by chain transitions at fixed solvent configuration (up to $5L^2$ time units). A typical run then consists of $5 \times 10^4$ iterations. We present below the results of numerical simulations of a chain length $L = 20$ in a solvent lattice of size $N = 100 \times 100$, for the temperature range $T = [0.25, 4]$ (here and in what follows, units are such that $k_B = 1$ and $J = 1$).

## III. RESULTS

We first calculate the potential of mean force that would be acting between a pair of solute molecules embedded in the model solvent. The potential of mean force is defined as the reversible work required to move two tagged solute molecules from an infinite separation to a separation $r$, so that any direct interaction between the two solutes has been subtracted [23]. The reversible work theorem states that if $\phi(r)$ is the direct interaction potential between two solute molecules separated by a distance $r$, and if $g(r)$ is the radial solute-solute pair correlation function, then the potential of mean force is $W(r) = -k_B T ln[g(r)e^{-\beta\phi(r)}]$. For the model at hand, one defines $P_{11}$ as the probability that two neighboring solvent molecules are in the state $S = +1$, and $P(r)$ as the probability that two pairs of neighboring solvent molecules in which their interstitial site is separated by a distance $r$ are in the state $S = +1$. If $\epsilon$ is the solute-solute interaction energy, the potential of mean force is

$$\beta W(r) = -ln\left[\frac{P(r)e^{-2\beta\epsilon}}{(P_{11}e^{-\beta\epsilon})^2}\right] = -ln\left[\frac{P(r)}{P_{11}^2}\right] \quad . \tag{2}$$

Note the cancellation of direct interaction terms involving $\epsilon$, and hence the potential of mean force in this model depends on the solvent only. The two phases of the solvent model are identified by the calculation of the magnetization of the lattice of solvent molecules, $m = \langle S \rangle$. At low temperatures, the solvent is in an ordered state (the liquid phase because of our initial condition), and $m = -1$, while at high temperature the solvent is in a disordered state $m = 0$. Our results for a range of temperatures are shown in Fig. 2. The force is always attractive, with a decreasing amplitude and increasing range with increasing temperature. These results are in agreement with those of Widom's group [24]. For reference, the inset of Fig. 2 also shows the magnetization $m$ and heat capacity $C_s$ of the solvent. The heat capacity is defined as

$$C_s = \frac{1}{Nk_BT^2}\langle \Delta E_s^2 \rangle = \frac{1}{Nk_BT^2}\left(\langle E_s^2 \rangle - \langle E_s \rangle^2\right) \qquad , \tag{3}$$

where $E_s$ is the energy of the solvent.

We next describe the results of the numerical simulation of the combined SARW and solvent system, and compare them with known results for a SARW in isolation. With solvent, a collapse transition is observed from a coil state at high temperature to a globular state at low temperature. However, the collapse transition temperature of the chain in solvent is higher than in isolation for the same value of $\epsilon$. We characterize the state of the chain by computing the radius of gyration,

$$\langle R_g^2 \rangle^{\frac{1}{2}} = \left\langle \frac{1}{2L^2} \sum_{i,j=1}^{L} (\mathbf{r}_i - \mathbf{r}_j)^2 \right\rangle^{\frac{1}{2}} \qquad , \tag{4}$$

and its derivative with respect to inverse temperature,

$$\left\langle R_g' \right\rangle = \left\langle \frac{\partial R_g}{\partial \beta} \right\rangle = \frac{1}{\left\langle R_g^2 \right\rangle}\left(\left\langle R_g^2 E_p \right\rangle - \left\langle R_g^2 \right\rangle \langle E_p \rangle\right). \tag{5}$$

Our results are shown in Figs. 3 (A,B). We observe collapse at $\theta_s \simeq 2$ for $H = 0$ and $H = -0.01$. The choice of $H < 0$ favors a bulk fluid phase within which chain collapse occurs with the nucleation of a vapor region ($S = +1$) as will be discussed in more detail below. If the magnitude of the field is too large, a sharp collapse transition is eliminated. For reference, the figure also shows our results for the SARW in isolation. In this latter case,

the radius of gyration is known to diverge as $L^{2\nu}$ and its derivative as $L^{\phi}$, where $\nu$ and $\phi$ are critical indices of the collapse transition. The temperature of the collapse transition is measured to be $\theta = 1.51 \pm 0.03$, with $\nu_\theta = 0.570 \pm 0.003$, and $\phi_\theta = 0.436 \pm 0.007$ (results not shown), in agreement with the exact value of those exponents [25], $\nu_\theta = 4/7$, and $\phi_\theta = 3/7$.

In solvent at low temperature, the self avoiding walk is in the collapsed state with the magnitude of the average radius of gyration and its derivative reduced as compared to the chain in isolation, as one would expect for a hydrophobic chain. By choice of initial conditions, the collapsed state is embedded in a bulk liquid phase ($S = -1$). Nevertheless, hydrophobic chain segments act as local positive magnetic fields, thus favoring the vapor phase ($S = 1$) in the vicinity of the chain. As the temperature is increased, we observe a sharp transition to a coil state which is accompanied by a transition from bulk liquid to bulk vapor in the solvent. This is the case both for $H = 0$ and $H < 0$ but small. Our results for the radius of gyration, its temperature derivative, and the second moment of energy fluctuations are shown in Fig. 3. For a chain length of $L = 20$, we observe a collapse transition at a temperature $\theta_s \simeq 2$, much higher that the collapse transition of the chain alone $\theta \simeq 1.52$. The value of $\theta_s$ has been estimated from the peak of the derivative of the radius of gyration with respect to temperature, which agrees with the value obtained from the fluctuations in total energy. The difference in collapse temperature can be directly attributed to the presence of the solvent. The figure also shows our results for $H = -0.1$, a stronger magnetic field favoring the liquid $S = -1$ phase. For this field intensity and higher, no collapse transition is observed below the order-disorder temperature of the solvent.

In order to further characterize the interplay between chain collapse and the structure of the solvent around it, we have calculated the following distribution function of the solvent

$$g(\mathbf{r} - \mathbf{r_{cm}}) = \langle S(\mathbf{r_{cm}}) S(\mathbf{r} - \mathbf{r_{cm}}) \rangle, \tag{6}$$

where $\mathbf{r_{cm}}$ is the center of mass of the SARW. Our results for the circularly averaged correlation function are shown in figure 4. At short distances from its center of mass, the chain is mostly immersed in vapor cells and the radial distribution function is $g(r - r_{cm}) \approx 1$ at all temperatures. On the other hand, a bulk liquid lattice at long distances from the center of mass corresponds to $g(r - r_{cm}) = -1$. We define the zero crossing of the correlation function to be a measure of the radius of the vapor domain surrounding the chain: $g(R_c) = 0$.

At $H = 0$ or small, and below the collapse transition temperature, the radial distribution function shows the existence of a vapor region immersed in the bulk liquid. At high temperature $T > T_c^{(s)}$, the critical temperature of the lattice solvent, the radial distribution is positive for all distances. The decay length decreases with increasing temperature as would be expected for a disordered medium. In the region of interest $\theta < T < T_c^{(s)}$, we observe a sharp transition around the collapse temperature $\theta_s \simeq 2$ for $L = 20$. For $T < \theta_s$, $R_c$ is finite and increases with temperature, becoming of order the size of our finite lattice at $\theta_s$. The insets of Fig. 4 show the linear dependence between the radius of the vapor domain $R_c$ and the radius of gyration of the chain $R_g$ for temperatures $T < \theta_s$. At $T = \theta_s$ $R_c$ becomes as large as our computational domain.

At low temperatures $T < \theta_s$, the lattice solvent is in the liquid phase. Immersion of hydrophobic particles is entropically unfavorable so that free energy minimization is achieved by increasing the number of contacts between monomers. The chain adopts a globular collapsed state. As the temperature increases, fluctuations leading to the formation of vapor sites in the bulk liquid increase which manifest themselves in a decrease in the amplitude of the potential of mean force but an increase in its range. We also observe an increase in the radius of the vapor domain with temperature that is proportional to the radius of gyration of the SARW. In the range $\theta < T < \theta_s$, whereas the SARW in a bulk vapor phase would be in its extended state, it is constrained here by the extent of the vapor domain $R_c$, and it adopts a collapse state instead. We also observe that $R_c$ diverges below $T_c^{(s)}$, as the local positive field created by the extended chain is sufficient to nucleate a vapor domain of the size of our computational system. At yet higher temperatures, the solvent is in a disordered state and there is no net solvent mediated potential of mean force acting on hydrophobic solute. There is no vapor domain in this temperature range, and the hydrophobic chain is in an extended coil state.

If the magnetic field $H$ is lower than approximately -0.1, we no longer observe a sharp collapse transition. Instead, we observe a smooth decrease of the radius of gyration with temperature. In this case, nucleation of a $S = +1$ region becomes energetically too costly, and the vapor domain remains small while surrounding a confined chain. If the temperature is increased, the critical temperature of the solvent $T_c^{(s)}$ is reached before the chain can unfold.

In summary, a weakly attractive self avoiding random walk (SARW) assumed to be hy-

drophobic, and embedded in a coarse grained lattice model of a solvent, undergoes a collapse transition at a temperature $\theta_s > \theta$, the SARW transition temperature in isolation. This temperature shift is attributed to solvent fluctuations. The collapse transition is accompanied by large fluctuations in the solvent, reflecting the growth of a depleted region around the collapsing chain. This effect is only present below the order-disorder transition temperature of the lattice solvent $T_c^{(s)}$.

The solvent model analyzed is equivalent to the large $Q$-state Potts model used by Ben-Naim and Widom and co-workers in their study of hydrophobicity. Advantages of the model are the possibility of obtaining analytic solutions for small solutes, and the computational simplicity afforded in our study of an embedded hydrophobic chain. However, at least for the range of SARWs studied ($L \leq 30$), and solvent lattices ($N \leq 10^4$), the extent of the vapor domain appears to diverge at the collapse temperature $\theta_s$. We do not observe a coil state inside a bulk liquid phase at any temperature below $T_c^s$. Although the large size of the vapor region observed at collapse is consistent with the related study of [9] concerning the free energy landscape for a different coarse grained model, this feature of our results may well be a finite size effect. It is also possible that it is related to the proximity between the collapse temperature and the critical point of the solvent in our model. In either case, we have been unable to find a range of negative $H$ that would stabilize an extended coil in a liquid phase of the solvent phase without preempting the collapse transition altogether.

**Acknowledgments**

This research has been supported by NSERC Canada. MG acknowledges further support by FQRNT. Computational resources have been provided by CLUMEQ.

---

[1] W. Still, A. Tempczyk, R. Hawley, and T. Hendrickson, J. Am. Chem. Soc. **112**, 6127 (1990).

[2] C. Tsai, S. Lin, H. Volfson, and R. Nussinov, Protein Sci. **6**, 53 (1997).

[3] R. Zhou and B. Berne, Proc. Natl. Acad. Sci. **99**, 12777 (2002).

[4] N. Nymeyer and E. Lindahl, Proc. Natl. Acad. Sci. **100**, 13934 (2003).

[5] V. Pande and E. Lindahl, Proc. Natl. Acad. Sci. **101**, 6456 (2004).

[6] E. Meyer, K. Rosenberg, and J. Israelachvili, Proc. Natl. Acad. Sci. **103**, 15739 (2006).

[7] I. Daidone, M. Ulmschneider, A. D. Noia, A. Amadei, and J. Smith, Proc. Natl. Acad. Sci. **104**, 15230 (2007).

[8] T. Miller, E. Vanden-Eijnden, and D. Chandler, Proc. Natl. Acad. Sci. **104**, 14564 (2007).

[9] P. ten Wolde and D. Chandler, Proc. Natl. Acad. Sci. **99**, 6539 (2002).

[10] D. Chandler, Nature **437**, 640 (2005).

[11] A. Ben-Naim, *Statistical Thermodynamics for Chemists and Biochemists* (Plenum, New York, 1992), pp. 220–223.

[12] A. Kolomeisky and B. Widom, Faraday Discuss. **112**, 81 (1999).

[13] P. Bhimalapuram, K. Koga, and B. Widom, Phys. Chem. Chem. Phys. **5**, 3085 (2003).

[14] G. Schutz, I. Ispolatov, G. Barkema, and B. Widom, Physica A **291**, 24 (2001).

[15] P. R. ten Wolde, S. X. Sun, and D. Chandler, Phys. Rev. E **65**, 0112011 (2002).

[16] L. Onsager, Phys. Rev. **65**, 117 (1944).

[17] E. Orlandini and T.Garel, Eur. Phys. J. B. **6**, 101 (1998).

[18] G. Parisi and N. Sourias, Phys. Rev. Lett. **45**, 871 (1981).

[19] A. Bortz, M. Kalos, and J. Lebowitz, J. Comp. Phys. **17**, 10 (1975).

[20] M. Lal, Molec. Phys. **17**, 57 (1969).

[21] N. Madras and A. D. Sokal, J. Stat. Phys. **50**, 109 (1988).

[22] N. Madras and G. Slade, *The Self-Avoiding Walk* (Birkhuser, Boston, 1993), p. 425.

[23] D. Chandler, *Introduction to modern statistical mechanics* (Oxford University Press, New York, 1987), p. 274.

[24] G. Barkema and B. Widom, J. Chem. Phys. **113**, 6 (2000).

[25] B. Duplantier and H. Saleur, Phys. Rev. Lett. **59**, 539 (1987).

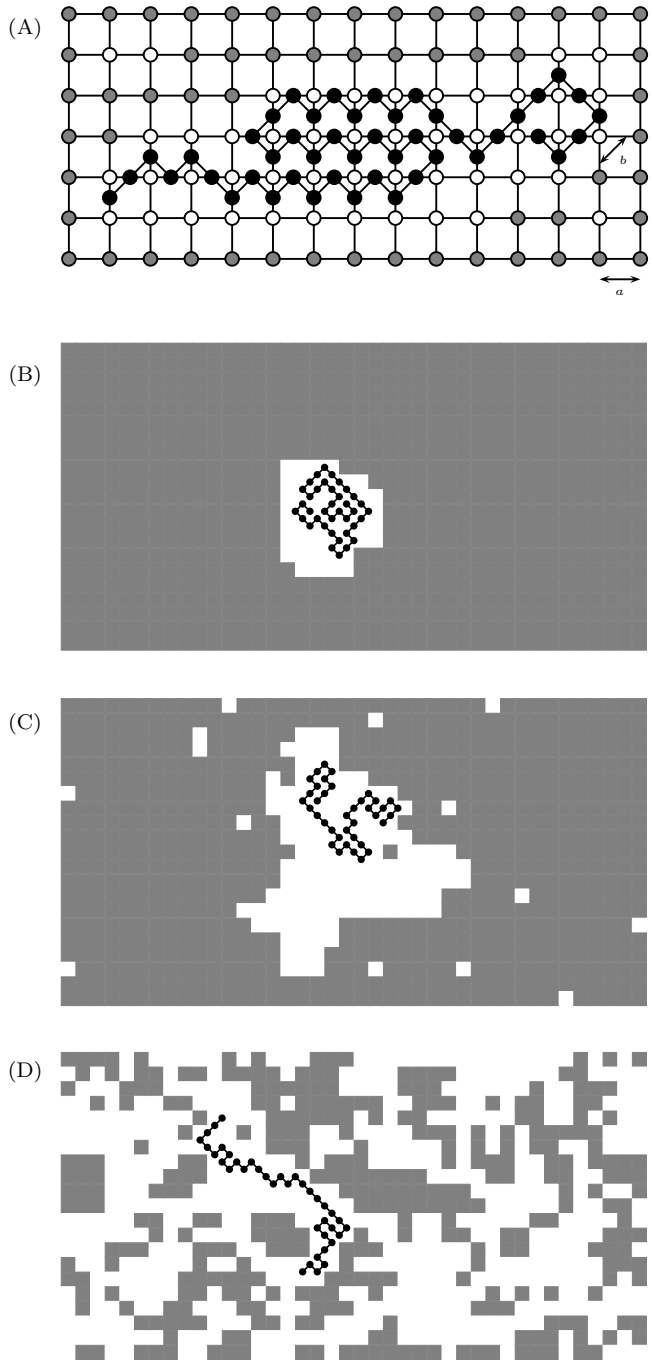


FIG. 1: (A). Schematic depiction of a chain conformation in the solvent lattice. Solvent cells occupy a two dimensional square lattice while the chain of monomers (the self avoiding random walk) is comprised of a sequence of nodes placed at interstitial sites in the square lattice (black circles). Hydrophobicity is modeled by the requirement that sites adjacent to each monomer be in the vapor ($S = 1$) state, shown in white in the figure. Cells occupied by liquid ($S = -1$) are colored gray. The parameters are $J = 1, H = 0$, and $\epsilon = -1$. (B). Example of a collapsed configuration at a temperature $T < \theta_s$, the collapse temperature in the presence of the solvent. (C). Configuration at the collapse temperature $T = \theta_s \simeq 2$, and, (D), an extended coil configuration at $T \gg \theta_s$.

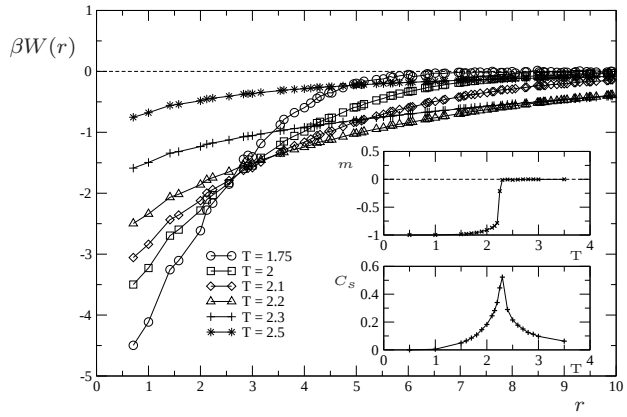


FIG. 2: Dimensionless potential of mean force $\beta W(r)$ acting on two solute particles a distance $r$ apart in units of the lattice spacing $a$, with $J = 1$ and $H = 0$, and a range of temperatures both below and above the collapse transition. The insets show the magnetization $m$ and the specific heat of the solvent $C_s$ obtained from numerical simulation for the same values of the parameters. The order-disorder transition of the solvent is $T_c^{(s)} \simeq 2.269$.

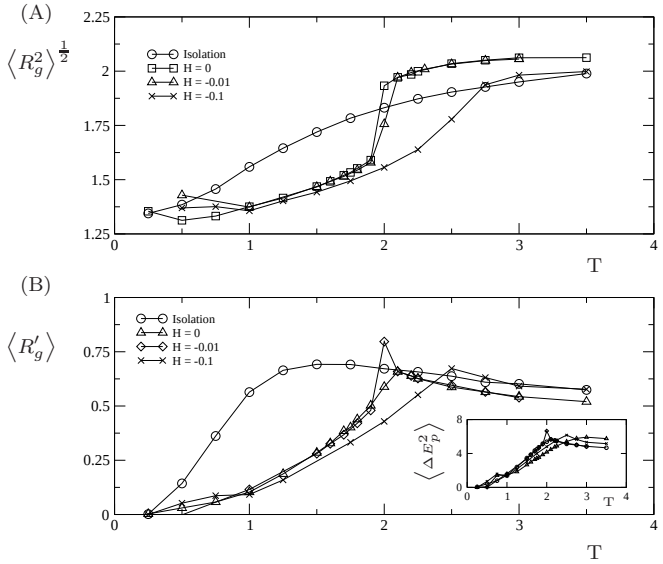


FIG. 3: Radius of gyration $\langle R_g^2 \rangle^{\frac{1}{2}}$ and its derivative $\langle R_g' \rangle$ as a function of temperature for a SARW of length $L = 20$. Shown are our results for no solvent, and for three magnetic field amplitudes $H = \{0, -0.01, -0.1\}$, with $J = 1$ and $\epsilon = -1$. The inset shows the temperature dependence of the fluctuations in chain energy ($\langle \Delta E_p^2 \rangle$). Other statistical measures of chain conformation (end to end distance and its derivative) show similar qualitative features and are not shown. The chain is in a globular collapsed state at low temperature and in an extended coil state at high temperature.

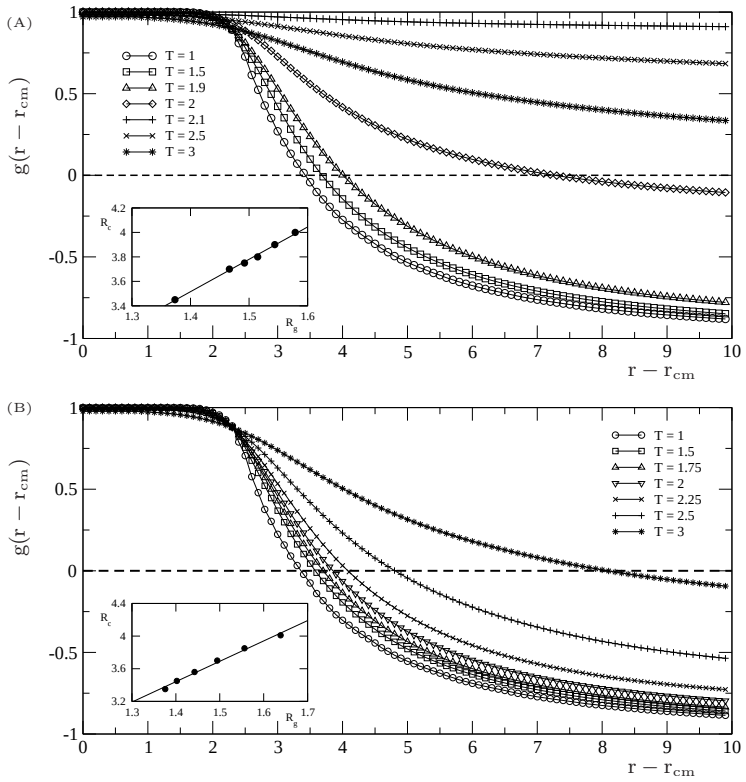


FIG. 4: Circularly averaged radial distribution function of the solvent $g(r-r_{cm})$ for a chain length $L = 20$ with $\epsilon = -1$, and $J = 1$, (A) $H = -0.01$, and (B) $H = -0.1$. The characteristic size of the vapor domain $R_c$ is determined by the zero crossing of the correlation function. As shown in Fig. 3, the chain in a field $H = -0.01$ exhibits a sharp collapse, but the chain at $H = -0.1$ does not. The inset shows the effective vapor radius $R_c$ as a function of the radius of gyration $\langle R_g^2 \rangle^{1/2}$. The radius $R_c$ scales linearly with $\langle R_g^2 \rangle^{1/2}$ indicating, in this model, the correlation between the growth of the vapor domain and the motion of the SARW that both creates the vapor domain and is effectively constrained to remain within it.